Assessing Martian Bulk Soil Hydration through Principal Component Analysis of Regional Chemical Data.
D. R. Hood[1], S. Karunatillake[2], and D. Susko[3], [1]Geology and Geophysics, LSU, Baton Rouge, LA 70803 (dhood7@lsu.edu) [2,3]Geology and Geophysics, LSU, Baton Rouge, LA 70803.

Introduction: Water has been detected on or near the Martian surface by a variety of instruments [1]–[4], however the nature of that water remains an open question. Solid H2O in the form of ice has been observed in northern and southern high latitudes by several instruments [5], [6] and by the phoenix lander in 2008 [7], it has also been suggested to occur in lower latitudes in the form of regolith mantled subsurface ice [8], [9]. H2O has also been observed to be a chemical constituent of minerals in both high latitudes [10] and equatorial regions [11]. There is even potential for transient liquid water in equatorial regions in the form of observed slope lineae [12], [13] and predicted perchlorate deliquescence brines [14]. Given that H2O is seen in such a variety of forms and settings, one must carefully assess the nature of H observed via remote sensing, where observations cannot always be placed in a specific geologic context. Observations from the GRS instrument provide a global picture of elemental abundances in the shallow subsurface of Mars. The variations seen at these depths (10s of centimeters) and spatial resolution ($5^O X 5^O$) are subtle, requiring extensive work to draw out only a few areas of interest [15]–[17]. While there are many multivariate methods that have been used in analyzing remote sensing data [17], previous work [16], [18], [19] has shown that Principal Component Analysis (PCA) is well suited for sensing subtle variations present in remote sensing and *in situ* data and localizing chemical anomalies. Here, PCA is used to assess the correlation between H_2O and other elements in the shallow subsurface of Mars. This is motivated in part by previous work [20], suggesting a meaningful correlation between H_2O and S in Martian regolith. This new analysis will further the previous work, investigating whether this correlation presents itself naturally in the data.

Methods: Currently, there are 9 elemental maps that have been generated from GRS data, Al, Ca, Fe, Cl, S, H (from which H_2O maps are derived), K, Th, and Si. These nine elemental datasets are combined with Ruff and Christensen's Dust Cover Index (DCI)[21] to form a 10-dimensinal dataset that covers all of mars, excluding the polar regions. To analyze our data, multivariate analysis techniques are applied to reduce the significant dimensionality of the data. Two of the most prominent methods available are Independent Component Analysis (ICA) [22] and Prinicipal Component Analysis (PCA) [16], [19], however we found that PCA was better suited to drawing out poten-

tial mineral components. The elemental distributions seen by the GRS instrument are roughly Gaussian [4], it follows that the mineral assemblages that generate these elemental signals are distributed in a Gaussian fashion. While ideal for drawing out non-gaussian components [17], ICA will disfavor Gaussian components, where PCA will generate components that are generally Gaussian, consistent with the expected distribution of hydrated minerals on Mars. PCA was implemented in the *Python* [23] language using *matplotlib* [24]. The primary result of PCA is 10 orthonormal axes, called Principal Components (PCs) that describe the data more succinctly than the original axes. In analyzing the GRS+DCI combined data, the first 2 PCs typically describe over 50% of the variance in the dataset. Therefore, our primary analyses is based on these two PCs in order to focus on bulk soil properties that are prevalent across regional scales. It is worth noting that it is difficult to gain extensive insight from individual principal components. In general, it is unlikely that any one PC will represent a certain mineral or even mineral assemblage. As such, covariance between two elements in one PC, or even in many PCs in one analysis is not sufficient to interpret a mineralogical correlation. For this reason, our analysis examines correlation between elements within PCs in both global analysis and sub-regional analyses.

*Error Incorporation.* To incorporate error, we chose to use the modified test parameter, t [15].

$$t_i = \frac{x_i - \bar{x}}{\sqrt{\sigma_i^2 + s^2}}$$

Where x_i is the mass fraction of a particular element in the *ith* bin, $\bar{x}$ is the average value of that element, σ_i is the error of the *ith* bin, and s is the standard deviation of the element distribution across the masked region (excluding poles). Processing the data before the PCA process allows the incorporation of error without modifying the standard PCA procedure.

Enriched and Depleted Zones. In our analysis PCA is applied to several subsets of the data. To separate these regions, a mask is applied to the "global" data, selecting regions that are above +1 or below -1 in terms of t-values, roughly representing 1 standard deviation above or below the mean. These enriched and depleted regions are used to identify chemically "atypical" regions of Mars. Examinations of these smaller regions will inform us of covariations at a local scale. These covariations are not necessarily representative of re-

gional properties, but occur in a more restricted geologic context. With the overall trends observed in global analyses, and the local variations observed in the enriched and depleted zones, we will be able to create an accurate picture of elemental covariance in soil at both scales

Similarity Analysis using the Dot Product. The PCA process projects the original data into a new, orthonormal space. In this space, Euclidian geometry and distance have similar meaning to that in typical 3-D space. Therefore, the angle between the vectors of a given element in PC-space can be used as a descriptor of the similarity of those two elements in PC-space. Elements with a small relative angle and a similar length in PC-space can be considered covarying. Similar comparisons were made by Gasnault et al. [16], however only in a qualitative fashion.
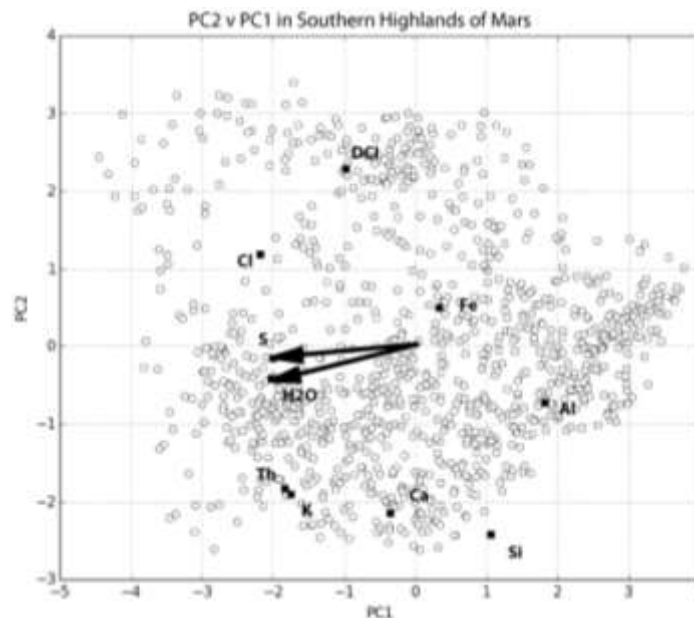
Figure 1. A biplot of PCA results from analysis on the Southern Highlands of Mars. White circles represent the elemental data projected into PC1 and PC2, black squares represent elemental axes projected into PC1 and PC2. Note the similarity in size and direction of the H_2O and S Vectors.

Discussion: In several settings on Mars strong correlations are observed between H and S. These correlations persist independent of the size, elemental composition, and geologic context of the analyzed regions. This suggests that, across the surface of mars, the concentration in H and S covary and are a significant control on variation in martian soil. We interpret this to show that a group of hydrated sulfate minerals have a strong effect on variation in soil composition across the surface of Mars and are the dominant reservoir of chemically-bound H_2O in martian soil. Across every

analyzed region, S is never more than 45 degrees away from H_2O, and only greater than 30 degrees in two regions. This suggests that apart from being consistently hydrated in the martian subsurface, sulfate minerals are the best candidate to be the primary hydrator. Previous work [20] has suggested, using molar ratios, that the correlation between H and S is well described using a variety of Fe-sulfates with H_2O:S ratios near 3:1. Unfortunately, two of the common sulfate cations detectable with GRS (Fe, Ca), lack strong correlations with H_2O. This lack of observed correlation may suggests that neither Fe-Sulfates, nor Ca-sulfates are the mineral of choice to describe the observed H_2O-S correlation. Mg-sulfates also provide appropriate H_2O:S ratios, however Mg remains undetectable by GRS, and cannot be incorporated into this analysis. Nevertheless, our results do not provide strong evidence toward or against any particular sulfate mineral candidate.

References: [1] W. C. Feldman, et al, J. Geophys. Res. E Planets, vol. 109, no. 9, pp. 1–13, 2004. [2] J. Audouard, et al, J. Geophys. Res. Planets, vol. 119, no. 8, pp. 1969–1989, 2014. [3] S. E. Ackiss et al, Icarus, vol. 243, pp. 311–324, Nov. 2014. [4] W. V. Boynton, et al, J. Geophys. Res., vol. 112, p. E12S99, Dec. 2007. [5] M. T. Mellon, et al, Icarus, vol. 169, no. 2, pp. 324–340, 2004. [6] M. Vincendon, et al, J. Geophys. Res. E Planets, vol. 115, no. 10, pp. 1–13, 2010. [7] S. Cull, et al, Geophys. Res. Lett., vol. 37, no. 24, p. n/a–n/a, Dec. 2010. [8] N. B. Karlsson, et al, Geophys. Res. Lett., p. n/a–n/a, 2015. [9] A. M. Bramson, et al, Geophys. Res. Lett., vol. 42, pp. 1–9, 2015. [10] M. H. Hecht, et al, Science (80-.)., no. July, 2009. [11] M. Nachon, et al, J. Geophys. Res. Planets, vol. 119, pp. 1991–2016, 2014.. [12] A. S. McEwen, et al, Nat. Geosci., vol. 7, no. 1, pp. 53–58, Dec. 2013. [13] L. Ojha, et al Geophys. Res. Lett., vol. 40, no. 1–6, p. GL057893, 2013. [14] F. J. Martín-Torres, et al, Nat. Geosci., no. April, pp. 1–5, 2015. [15] S. Karunatillake, et al, J. Geophys. Res., vol. 114, no. E12, p. E12001, Dec. 2009. [16] O. Gasnault, et al, Icarus, vol. 207, no. 1, pp. 226–247, May 2010. [17] A. D. Rogers et al, J. Geophys. Res. Planets, vol. 120, no. 1, pp. 62–91, 2014. [18] D. R. Klassen, Icarus, vol. 204, no. 1, pp. 32–47, 2009. [19] E. Jones, J. Geophys. Res. Planets, pp. 1023–1043, 2015. [20] S. Karunatillake, et al Geophys. Res. Lett., vol. 41, no. 22, pp. 7987–7996, 2014. [21] S. W. Ruff et al, J. Geophys. Res., vol. 107, no. E12, p. 5127, 2002. [22] A. Hyvärinen et al, Neural Networks, vol. 13, no. 4–5, pp. 411–430, 2000. [23] G. van Rossum, "Python Tutorial, Technical Report CS-R9526," Amsterdam, 1995. [24] J. D. Hunter, Comput. Sci. Eng., vol. 9, no. 3, pp. 90–95, 2007.